Austenite–martensite interface in shape memory alloys

C. H. Lei,[1] L. J. Li,[1] Y. C. Shu,[2] and J. Y. Li[1,a)]
[1]*Department of Mechanical Engineering, University of Washington, Seattle, Washington 98195-2600, USA*
[2]*Institute of Applied Mechanics, National Taiwan University, Taipei 106, Taiwan*

(Received 8 February 2010; accepted 14 March 2010; published online 9 April 2010)

A two-scale phase field simulation is developed for austenite–martensite interface to understand the effects of crystalline symmetry and geometric compatibilities on the reversibility of structural phase transformations in shape memory alloys. It is observed that when the middle eigenvalue of martensite transformation strain is equal to zero, an exact austenite–martensite interface is formed with negligible elastic energy. On the other hand, when the middle eigenvalue is different from 0, an inexact interface between austenite and martensitic twin is formed, and the corresponding elastic energy increases with the increased magnitude of the middle eigenvalue, resulting in substantially higher energy barrier for austenite–martensite transformation, and thus higher thermal hysteresis in shape memory alloys. © *2010 American Institute of Physics*. [doi:10.1063/1.3385278]

The reversibility of structural phase transformations has not only long-standing theoretical interests in condensed matter physics, but also profound technological implications for a wide range applications, ranging from fatigue life of shape memory alloys[1] to magnetoelectric coupling in multiferroic oxides.[2,3] It has recently been postulated that the reversibility of structural phase transformations, as manifested by their hysteresis characteristics, critically depends on the crystalline symmetry and geometric compatibilities of austenite and martensite phases.[4–6] When the middle eigenvalue of the transformation matrix of the martensite lattice with respect to the austenite structure equals 1, a compatible interface between these two phases can be formed, and it was suggested that the corresponding thermal hysteresis of shape memory alloys will be minimized.[5,6] This principle has been used to guide the search for shape memory alloys with extremely low hysteresis, and a clear relationship between the thermal hysteresis and the middle eigenvalue as expected from the theory has been observed.[1,5,6]

When the middle eigenvalue of the transformation matrix is different from 1, a compatible austenite–martensite interface is no longer possible. Instead, interfaces between austenite phase and twined martensite are observed, which satisfy the compatibility condition on average.[6–9] This leads to increased elastic energy due to the incompatibility between the austenite and martensite phases, resulting in higher energy barrier for phase transformation and thus higher thermal hysteresis. Indeed, an analytic model based on an inexact interface with an assumed transition layer between austenite and twined martensite yields a relationship between thermal hysteresis and middle eigenvalue that resembles experimental observations.[1,6] The analysis, however, depends on the transition layer assumed. To understand the detailed structure of austenite–martensite interface and its implication on thermal hysteresis of shape memory alloys, especially when the middle eigenvalue of transformation matrix deviates from 1, direct numerical simulation without making any prior assumption on the underlying microstructure is highly desirable, which we seek to develop in this letter using phase field approach.[10–14]

To this end, we adopt a geometric linear theory,[15] which uses transformation strains instead of transformation matrices to characterize the martensitic structure with respect to the austenite reference, and as such, the middle eigenvalue of transformation matrix equalling 1 in finite deformation theory corresponds to the middle eigenvalue of transformation strain equalling 0 in geometric linear theory. To be specific, we consider two martensitic variants with transformation strains $\boldsymbol{\varepsilon}^{(1)}$ and $\boldsymbol{\varepsilon}^{(2)}$, which are assumed to be compatible with each other, satisfying[7]

$$\boldsymbol{\varepsilon}^{(1)} - \boldsymbol{\varepsilon}^{(2)} = \tfrac{1}{2}(\mathbf{a} \otimes \mathbf{n} + \mathbf{n} \otimes \mathbf{a}), \tag{1}$$

making it possible to form a martensitic twin with these two variants, where $\mathbf{n}$ is the normal of twin interface, and $\mathbf{a}$ is related to the shear of the twin structure. By definition, the transformation strain of the austenite phase is 0, and in order for a compatible austenite–martensite interface to be formed, the middle eigenvalue of the transformation strain $\boldsymbol{\varepsilon}^{(i)}$ of martensitic variant has to be 0. This turns out to be a very restrictive condition, and is not satisfied in general.[7] Instead, the averaging transformation strain $\mu_2\boldsymbol{\varepsilon}^{(1)}+(1-\mu_2)\boldsymbol{\varepsilon}^{(2)}$ of a martensitic twin structure can have zero middle eigenvalue when appropriate volume fraction μ_2 is chosen, suggesting an inexact interface between austenite and martensitic twin,[7] such that

$$\mu_2\boldsymbol{\varepsilon}^{(1)} + (1-\mu_2)\boldsymbol{\varepsilon}^{(2)} = \tfrac{1}{2}(\mathbf{b} \otimes \mathbf{m} + \mathbf{m} \otimes \mathbf{b}), \tag{2}$$

where $\mathbf{m}$ is the normal of the inexact interface, and $\mathbf{b}$ is the corresponding shear, as schematically shown in Fig. 1. In general, two sets of solutions for Eq. (2) exist, corresponding to two possible interfaces with specific normal and volume fractions of the martensitic twins.

To confirm that an inexact interface between austenite and twined martensite can indeed be formed as schematically shown in Fig. 1, an unconventional phase field approach is developed.[16–21] Two characteristic functions $\mu_1(\mathbf{x})$ and $\mu_2(\mathbf{x})$ are introduced as the field variables to define the structure, such that $\mu_1(\mathbf{x})$ takes value of 1 if $\mathbf{x}$ is occupied by austenite phase and 0 if it is occupied by either of the martensitic variants, whose specification is governed by $\mu_2(\mathbf{x})$, which

a)Author to whom the correspondence should be addressed. Electronic mail: jjli@u.washington.edu.

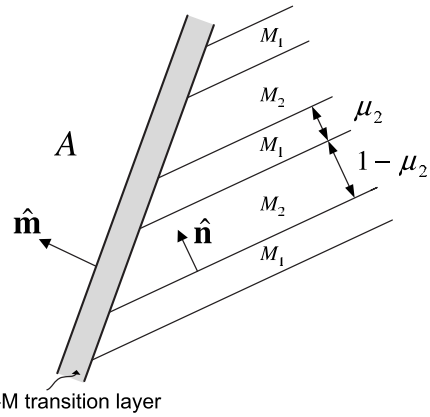

FIG. 1. The schematics of an inexact interface between austenite (a) and martensitic twin (M_1 and M_2).

takes the value of 1 if **x** is occupied by variant 1 and 0 if it is occupied by variant 2. As a result, the transformation strain at **x** is given by

$$\boldsymbol{\varepsilon}^*[\boldsymbol{\mu}] = (1-\mu_1)\mu_2\boldsymbol{\varepsilon}^{(1)} + (1-\mu_1)(1-\mu_2)\boldsymbol{\varepsilon}^{(2)}, \tag{3}$$

where $\boldsymbol{\mu}=[\mu_1,\mu_2]$. Note that while μ_2 is governed by Eq. (2), μ_1 is generally determined by the mechanical boundary condition. For an arbitrary distribution of $\boldsymbol{\mu}(\mathbf{x})$, this transformation strain might not be compatible, and an elastic field will be induced, resulting in elastic energy in the structure,

$$W^{\text{ela}}(\boldsymbol{\mu}) = \tfrac{1}{2}(\boldsymbol{\varepsilon} - \boldsymbol{\varepsilon}^*|\boldsymbol{\mu}|) \cdot \mathbf{C}(\boldsymbol{\varepsilon} - \boldsymbol{\varepsilon}^*|\boldsymbol{\mu}|), \tag{4}$$

where $\boldsymbol{\varepsilon}$ is the total strain that can be solved from mechanical equilibrium equation, consisting of elastic strain and transformation strain, and **C** is the elastic stiffness tensor. To ensure that μ_1 and μ_2 take either 1 or 0, an anisotropy energy is introduced,

$$W^{\text{ani}}(\boldsymbol{\mu}) = K_1\mu_1^2(1-\mu_1)^2 + K_2\mu_2^2(1-\mu_2)^2, \tag{5}$$

where K_1 and K_2 are the anisotropy constants. In addition, interfacial energy is introduced to penalize gradients in the characteristic functions, such that

$$W^{\text{gra}}(\boldsymbol{\mu}) = A|\nabla\boldsymbol{\mu}|^2. \tag{6}$$

The potential energy of the system is then given by

$$\mathcal{I}(\boldsymbol{\mu}) = \int_\Omega [W^{\text{gra}}(\boldsymbol{\mu}) + W^{\text{ani}}(\boldsymbol{\mu}) + W^{\text{ela}}(\boldsymbol{\mu}) - \boldsymbol{\sigma}^0 \cdot \boldsymbol{\varepsilon}]d\mathbf{x}, \tag{7}$$

where Ω is the domain occupied by the shape memory alloy, and $\boldsymbol{\sigma}^0$ is the stress arising from the traction applied at the boundary. The variation in potential energy with respect to $\boldsymbol{\mu}$ results in the driving force for the evolution of $\boldsymbol{\mu}$,

$$\mathbf{F}(\boldsymbol{\mu}) = -\frac{\delta\mathcal{I}(\boldsymbol{\mu})}{\delta\boldsymbol{\mu}} = \mathbf{F}^{\text{gra}}(\boldsymbol{\mu}) + \mathbf{F}^{\text{ani}}(\boldsymbol{\mu}) + \mathbf{F}^{\text{ela}}(\boldsymbol{\mu}), \tag{8}$$

and under a linear kinetic approximation, the evolution equation for $\boldsymbol{\mu}$ is derived as

$$\frac{\partial\boldsymbol{\mu}}{\partial t} = M[\mathbf{F}^{\text{gra}}(\boldsymbol{\mu}) + \mathbf{F}^{\text{ani}}(\boldsymbol{\mu}) + \mathbf{F}^{\text{ela}}(\boldsymbol{\mu})], \tag{9}$$

where M is the linear evolution coefficient, and $\mathbf{F}^{\text{ani}}(\boldsymbol{\mu}) = -\partial W^{\text{ani}}(\boldsymbol{\mu})/\partial\boldsymbol{\mu}$, $\mathbf{F}^{\text{gra}}(\boldsymbol{\mu}) = 2A\nabla^2\boldsymbol{\mu}$, and $\mathbf{F}^{\text{ela}}(\boldsymbol{\mu}) = \boldsymbol{\sigma}\cdot\partial\boldsymbol{\varepsilon}^*[\boldsymbol{\mu}]/\partial\boldsymbol{\mu}$.

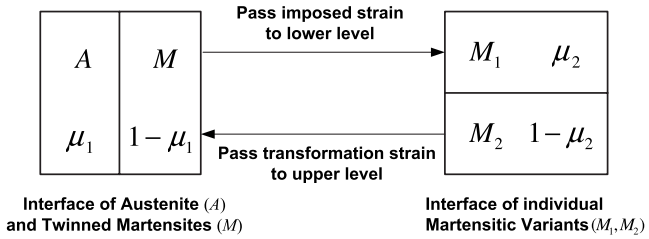

FIG. 2. The schematics of two-scale simulation for austenite–martensite interface.

The theory is implemented into a numerical simulation on a x_1-x_2 plane whose normal is defined by $\mathbf{m}\times\mathbf{n}$, and all the field variables are assumed to be independent of x_3. Thus a two-dimensional simulation will be sufficient, though all the tensorial variables are three-dimensional in nature. From the definition of μ_1 and μ_2, it is clear that μ_1 represents austenite–martensite structure, while μ_2 represents martensitic twin within the austenite–martensite structure. As a result, the length scales involved in μ_1 and μ_2 are clearly different. A two-scale simulation scheme is adopted to reflect such difference, where μ_1 and μ_2 are simulated at two distinct length scales, yet are coupled together through boundary condition and distribution of transformation strain, as schematically shown in Fig. 2. At upper scale where μ_1 is evolved, μ_2 is assumed to be fixed, and it specifies the transformation strain of the martensite through Eq. (3). On the other hand, at lower scale where μ_2 is evolved, μ_1 is assumed to be fixed, and the boundary condition on the lower scale simulation cell is specified by the average strain in the martensite calculated at upper scale. The simulation starts with random initial conditions for μ_1 and μ_2 at both scales, and iterations between these two scales continue until a stable configuration emerges. To solve for Eq. (9) at either scale, fast Fourier transform[22] is adopted on spatial scale with 128×128 cell size, and semi-implicit finite difference scheme[11] is adopted on temporal scale with a time step of 0.005. The elastic constants of the material are assumed to be $C_{11}=80\times10^9$ Pa, $C_{12}=20\times10^9$ Pa, and $C_{66}=30\times10^9$ Pa.

The phase field simulation is applied to study austenite–martensite interface for a cubic-to-orthorhombic transformation, which has transformation strains given by

$$\boldsymbol{\varepsilon}^{(1)} = \begin{pmatrix} \alpha & 0 & \gamma \\ 0 & \beta & 0 \\ \gamma & 0 & \alpha \end{pmatrix}, \quad \boldsymbol{\varepsilon}^{(2)} = \begin{pmatrix} \alpha & 0 & -\gamma \\ 0 & \beta & 0 \\ -\gamma & 0 & \alpha \end{pmatrix}. \tag{10}$$

We focus on the volume-preserving transformation, which is a necessary condition for self-accommodating structure.[7,23] As a result, we have $\beta=-2\alpha$, and the three eigenvalues are given by $\{-2\alpha,\alpha-\gamma,\alpha+\gamma\}$. When the middle eigenvalue is set to be 0, a sharp austenite–martensite interface emerges from the simulation, as shown in Fig. 3(a), and the normal of the interface is indeed what we expect from the geometric linear theory. When the middle eigenvalue is different from 0, then such an exact interface is no longer possible, and a typical austenite–martensite structure obtained in the simulation is shown in Fig. 3(b), where a rough interface between austenite and martensitic twin is observed. The martensitic twin has interface normal and volume fraction expected from Eqs. (1) and (2), while the austenite–martensite interface, though rugged, has an average interface normal that is consistent with Eq. (2). So the simulation we developed can

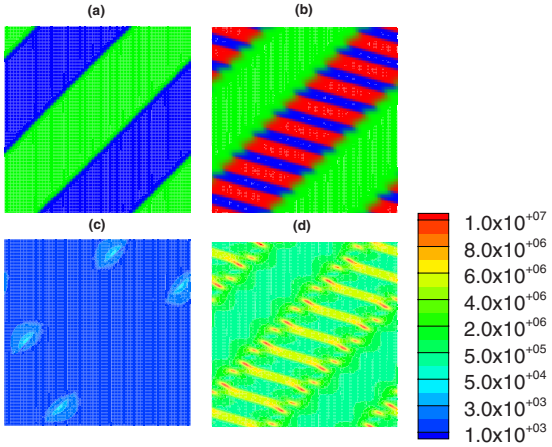

FIG. 3. (Color online) Austenite–martensite interfaces by phase field simulation; (a) compatible interface when the middle eigenvalue of the transformation strain is 0 and (b) inexact interface when the middle eigenvalue of the transformation strain is not 0; (c) and (d) the corresponding distribution of elastic energy in the structure, with the scale bar indicating the elastic energy density.

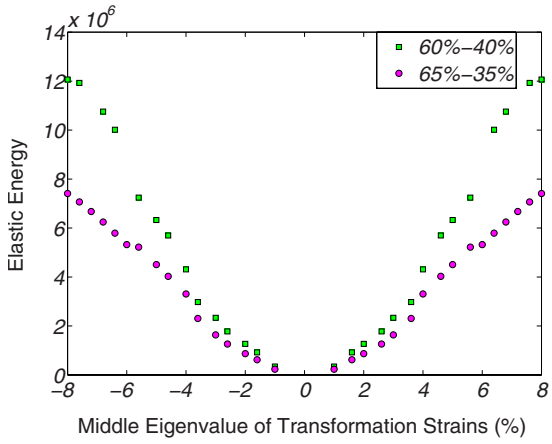

FIG. 4. (Color online) The elastic energy as function of middle eigenvalue of the transformation strain for volume-preserving transformation.

indeed capture the austenite–martensite interface, and can reveal the detailed interfacial structure without any prior assumption. There is indeed a transition layer between austenite and martensitic twin, as suggested before, due to the incompatibility between austenite and martensite phases. The zigzag type of interface in the transition layer is also consistent with certain experimental observations, and we are working on to capture the fine-scaled branching martensite twins often observed near the interface.[7]

The incompatible interface is expected to result in higher internal stress, and thus higher elastic energy, and the necessity of martensitic twin for an averaging compatible interface should also result in higher interfacial energy. This is indeed what we observe in the simulation. The distributions of elastic energy corresponding to the austenite–martensite structures in Figs. 3(a) and 3(b) are shown in Figs. 3(c) and 3(d). Negligible elastic energy is observed for the exact austenite–martensite interface, as expected. On the other hand, stress concentration is observed near the inexact austenite–martensite interface due to the incompatibility of the austenite and martensite phases, resulting in much higher elastic energy, as shown in Fig. 3(d). Such stress concentration and higher elastic energy will result in higher energy barrier for austenite–martensite phase transformation, and consequently higher thermal hysteresis. To appreciate this, we simulate the austenite–martensite interfaces for a range of middle eigenvalues of the transformation strains, and calculate the corresponding total elastic energy in the structures, as shown in Fig. 4. Two types of martensitic twin are considered, one with volume fraction of 60%, and the other 65%. Notice that different volume fractions of martensitic variants under a fixed middle eigenvalue is possible, since the volume preserving orthorhombic transformation strain has two independent variables α and γ. It is observed that in both structures the elastic energy increases as the middle eigenvalues deviate from 0, suggesting an increased energy barrier and thus higher thermal hysteresis, as observed in recent experiments.[1,5,6] The simulation thus is able to explain the thermal hysteresis in shape memory alloys as related to the crystalline symmetry of austenite and martensite phases, and we are currently developing phase field simulation of austenite–martensite transformation, which would allow us to quantify the thermal hysteresis directly.

We gratefully acknowledge the support of U.S. ARO (Grant No. W911NF-07-1-0410) and NSF Metal program (Grant No. DMR-0631687). Y.C.S. is also supported by TW NSC (Grant No. 97-2221-E-002-125-MY3).

[1] J. Cui, Y. S. Chu, O. O. Famodo, Y. Furuya, J. Hattrick-Simpers, R. D. James, A. Ludwig, S. Thienhaus, M. Wuttig, Z. Zhang, and I. Takeuchi, Nature Mater. **5**, 286 (2006).
[2] Y. H. Chu, L. W. Martin, M. B. Holcomb, M. Gajek, S. J. Han, Q. He, N. Balke, C. H. Yang, D. Lee, W. Hu, Q. Zhan, P. L. Yang, A. Fraile-Rodriguez, A. Scholl, S. X. Wang, and R. Ramesh, Nature Mater. **7**, 478 (2008).
[3] T. Zhao, A. Scholl, F. Zavaliche, K. Lee, M. Barry, A. Doran, M. P. Cruz, Y. H. Chu, C. Ederer, N. A. Spaldin, R. R. Das, D. M. Kim, S. H. Baek, C. B. Eom, and R. Ramesh, Nature Mater. **5**, 823 (2006).
[4] K. Bhattacharya, S. Conti, G. Zanzotto, and J. Zimmer, Nature (London) **428**, 55 (2004).
[5] R. D. James and Z. Zhang, *Magnetism and Structure in Functional Materials* (Springer, Berlin, 2005), Vol. 79.
[6] Z. Zhang, R. D. James, and S. Mueller, Acta Mater. **57**, 4332 (2009).
[7] K. Bhattacharya, *Microstructure of Martensite: Why it Forms and How it Gives Rise to the Shape-Memory Effect* (Oxford University, New York, 2003).
[8] Z. Xiangyang, S. Qingping, and Y. Shouwen, J. Mech. Phys. Solids **48**, 2163 (2000).
[9] Q. P. Sun, T. T. Xu, and X. Y. Zhang, ASME J. Eng. Mater. Technol. **121**, 38 (1999).
[10] J. X. Zhang and L. Q. Chen, Philos. Mag. Lett. **85**, 533 (2005).
[11] L. Q. Chen, Annu. Rev. Mater. Res. **32**, 113 (2002).
[12] Y. H. Wen, L. Q. Chen, P. M. Hazzledine, and Y. Wang, Acta Mater. **49**, 2341 (2001).
[13] A. Artemev, Y. Jin, and A. G. Khachaturyan, Acta Mater. **49**, 1165 (2001).
[14] Y. Wang and A. G. Khachaturyan, Acta Mater. **45**, 759 (1997).
[15] K. Bhattacharya, Continuum Mech. Thermodyn. **5**, 205 (1993).
[16] L. J. Li, J. Y. Li, Y. C. Shu, and J. H. Yen, Appl. Phys. Lett. **93**, 192506 (2008).
[17] L. J. Li, J. Y. Li, Y. C. Shu, H. Z. Chen, and J. H. Yen, Appl. Phys. Lett. **92**, 172504 (2008).
[18] Y. C. Shu, J. H. Yen, H. Z. Chen, J. Y. Li, and L. J. Li, Appl. Phys. Lett. **92**, 052909 (2008).
[19] Y. C. Shu and J. H. Yen, Acta Mater. **56**, 3969 (2008).
[20] Y. C. Shu and J. H. Yen, Appl. Phys. Lett. **91**, 021908 (2007).
[21] L. Yang and K. Dayal, Appl. Phys. Lett. **96**, 081916 (2010).
[22] D. Kopriva, *Implementing Spectral Methods for Partial Differential Equations* (Springer, Berlin, 2009).
[23] K. Bhattacharya, Arch. Ration. Mech. Anal. **120**, 201 (1992).